

See discussions, stats, and author profiles for this publication at: <https://www.researchgate.net/publication/259954312>

Sediment Contaminated with the Azo Dye Disperse Yellow 7 Alters Cellular Stress- and Androgen-Related Transcription in *Silurana tropicalis* Larvae

ARTICLE *in* ENVIRONMENTAL SCIENCE & TECHNOLOGY · JANUARY 2014

Impact Factor: 5.33 · DOI: 10.1021/es500263x · Source: PubMed

CITATIONS

8

READS

45

5 AUTHORS, INCLUDING:



[Shane R De Solla](#)

Environment Canada

57 PUBLICATIONS 934 CITATIONS

[SEE PROFILE](#)



[Vimal K Balakrishnan](#)

Environment Canada

27 PUBLICATIONS 645 CITATIONS

[SEE PROFILE](#)

Sediment Contaminated with the Azo Dye Disperse Yellow 7 Alters Cellular Stress- and Androgen-Related Transcription in *Silurana tropicalis* Larvae

Justine Mathieu-Denoncourt,[†] Christopher J. Martyniuk,^{‡,§} Shane R. de Solla,[§] Vimal K. Balakrishnan,^{||} and Valérie S. Langlois^{†,*}

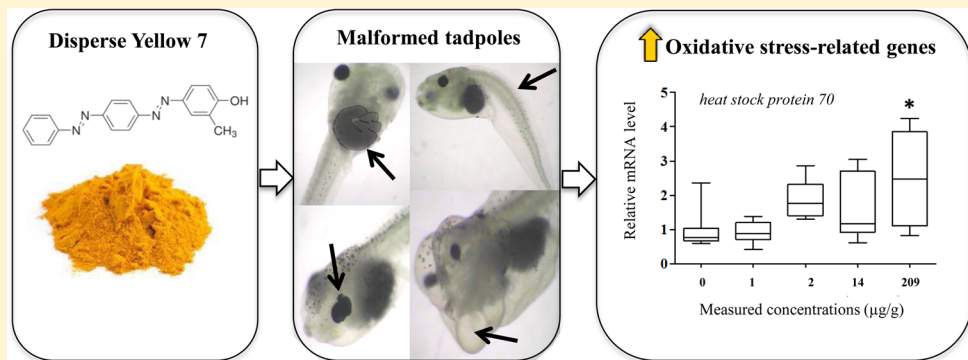
[†]Chemistry and Chemical Engineering Department, Royal Military College of Canada, Kingston, Ontario, Canada K7K 7B4

[‡]University of New Brunswick and Canadian Rivers Institute, New Brunswick, Canada E2L 4L5

[§]Wildlife and Landscape Science Directorate, Environment Canada, Burlington, Ontario, Canada L7R 4A6

^{||}Aquatic Contaminants Research Division, Water Science and Technology Directorate, Environment Canada, Burlington, Ontario, Canada L7R 4A6

Supporting Information



ABSTRACT: Azo dyes are the most commonly used type of dye, accounting for 60–70% of all organic dye production worldwide. They are used as direct dyes in the textile, leather, printing ink, and cosmetic industries. The aim of this study was to assess the lethal and sublethal effects of the disazo dye Disperse Yellow 7 (DY7) in frogs to address a knowledge gap regarding mechanisms of toxicity and the potential for endocrine disrupting properties. Larvae of *Silurana tropicalis* (Western clawed frog) were exposed to DY7-contaminated water (0 to 22 $\mu\text{g/L}$) and sediment (0 to 209 $\mu\text{g/g}$) during early larval development. The concentrations used included the range of similar azo dyes found in surface waters in Canada. A significant decrease in tadpole survivorship was observed at 209 $\mu\text{g/g}$ while there was a significant increase in malformations at the two highest concentrations tested in sediment. In the 209 $\mu\text{g/g}$ treatment, DY7 significantly induced *hsp70* (2.5-fold) and *hsp90* (2.4-fold) mRNA levels, suggesting that cells required oxidative protection. The same treatment also altered the expression of two androgen-related genes: decreased *ar* (2-fold) and increased *srd5a2* (2.6-fold). Furthermore, transcriptomics generated new hypotheses regarding the mechanisms of toxic action of DY7. Gene network analysis revealed that high concentrations of DY7 in sediment induced cellular stress-related gene transcription and affected genes associated with necrotic cell death, chromosome condensation, and mRNA processing. This study is the first to report on sublethal end points for azo dyes in amphibians, a growing environmental pollutant of concern for aquatic species.

INTRODUCTION

Azo dyes have been used for over a century as direct dyes in the textile, leather, printing ink, and cosmetic industries¹ with approximately 800 000 tons of dye being produced worldwide yearly.² Azo compounds are diazenes possessing either aryl or alkyl groups (e.g., R—N=N—R'), although aryl azo compounds are more common than aliphatic azo compounds. Chromophores are linked to the azo bonds and give the color to the molecule. Industrial effluents contaminated with azo dyes have a strong color, a high chemical oxygen demand, and low biodegradability.² It is estimated that between 10 and 15% of

azo dyes are released into aquatic systems as effluent.¹ Land application of sewage sludge is a secondary route through which azo dyes enter terrestrial ecosystems. Many azo dyes are not degraded during conventional treatment of industrial effluents,³ and many remain unchanged after they pass through activated sludge systems.⁴ Furthermore, it has been found that the total concentration of organic dyes can be as high as 456.2

Received: June 24, 2013

Accepted: January 27, 2014

Published: January 27, 2014



$\mu\text{g/g}$ in surface soil near synthetic dye industries.⁵ Few studies have measured azo dyes in Canadian surface waters, or surficial or suspended sediment. However, in a 1987–1989 survey of the Yamaska River (Quebec), Disperse Blue 26, Disperse Blue 79, and Disperse Red 60, as well as 1 azo metabolite and 12 unidentified dyes, were detected in water with concentrations ranging from 3 to 17 $\mu\text{g/L}$.⁶

The importance of conducting environmental risk assessments for azo compounds has been recognized by several countries. In 2006, the Government of Canada introduced the Chemicals Management Plan (CMP) as part of its objective to rigorously assess the environmental risks associated with a variety of chemical substances. Aromatic azo and benzidine-based substances commonly used as dyes were among the groups of chemicals targeted by the CMP, with disperse azo dyes accounting for 73 compounds on the list. Azo compounds are also being evaluated in the European Union using the registration, evaluation, authorization, and restriction of chemicals (REACH) regulations (EC 1907/2006), and by the United States Environmental Protection Agency (US EPA).

In support of the environmental risk assessment activities to address the health effects of azo dyes, developing Western African frog (*Silurana tropicalis*) larvae were exposed to either Disperse Yellow 7 (DY7)-contaminated water or sediment to assess its toxicity and to measure sublethal effects resulting from chemical treatment. Mortality of larvae and deformities were quantified, and further investigation was conducted to understand the mechanisms of action by which DY7 triggers its toxic effects using two approaches: (1) focused analysis using qPCR to investigate heat shock proteins and endocrine-related genes and (2) transcriptome-wide microarray investigation followed by gene network analysis to better characterize mechanisms of action of DY7.

MATERIALS AND METHODS

Reagents and solutions. DY7 (purity 95%; CAS 6300-37-4) was purchased from Sigma Canada Ltd. (Oakville, CA). The Frog Embryo Teratogenesis Assay-*Xenopus* (FETAX) solution consisted of 625 mg NaCl, 96 mg NaHCO₃, 75 mg MgSO₄, 60 mg CaSO₄·2H₂O, 30 mg KCl, and 15 mg CaCl₂/L of deionized, distilled water.⁷

Animals and Breeding. Adult *S. tropicalis* frogs were reared in dechlorinated and aerated water from Queen's University Animal Care Facility (Kingston, ON). Breeding was performed according to Langlois et al., 2010.⁸ Eggs were collected and kept in FETAX solution with 0.04 ppm of the antibiotic gentamicin sulfate. Embryos were dejellied to facilitate handling by gently swirling the egg masses for 2 min in 2% w/v L-cysteine solution prepared with FETAX solution (pH 8.1).

Experimental Design. Since Fort et al. (2004) showed that *S. tropicalis* is a suitable alternative species for *Xenopus laevis* in FETAX assays,⁹ a modified version of the FETAX⁷ whole embryo assay was developed to evaluate the developmental toxicity of DY7 in *S. tropicalis* embryos. FETAX solution was kept at 25 \pm 1 °C and renewed every 24 h to ensure that oxygen levels remained high and to maintain optimal water quality conditions. Lighting was maintained at a 12 h light and 12 h dark cycle starting at 7:00 A.M. At 24, 48, and 72 h, dead embryos were removed to avoid microbial growth.⁷ The number of dead embryos per jar was recorded daily. Each replicate contained 40 embryos. Gentamicin sulfate was added to every jar prior to the beginning of the test (Sandoz Canada,

Inc., Boucherville, QC).¹⁰ Two sets of exposures were carried out using DY7: (1) exposure to contaminated water (0, 1, 5, 7, and 22 $\mu\text{g/L}$) and (2) exposure to contaminated sediment (0, 1, 2, 14, and 209 $\mu\text{g/g}$). For the waterborne experiment, DY7 was dissolved in 0.7% (v/v) DMSO, whereas MEOH was used to spike the sediment. The two assays were conducted with larvae at Nieuwkoop-Faber (NF) developmental stages 11 (10 h postfertilization) to 46 (72 h postfertilization). Embryos were added to 96-mL of FETAX solution in small mason jars (Bernardin, Richmond Hill, ON). For both experiments, exposure and control treatments had four or six replicates.

In the sediment exposure experiment, a total of 24 g of sediment collected from Lake Erie (Canada) was poured into each jar and then placed in the dark at 4 °C until needed. Background chemistry was performed on sediment to ascertain that all organic contaminants and metals measured were below the lowest effect levels and probable effects.¹¹ A day prior to the beginning of the exposure, 96 mL of FETAX solution was added to each jar, representing a 1:4 dilution of sediment to water. The loading density was 1 g/L, which is the density required for larvae to grow at a normal rate.^{7,9} The sediment was allowed to settle for 24 h before the addition of larvae. Gentamicin sulfate (96 μL) was added to the solution prior to the introduction of the animals. Egg holders were designed to prevent the eggs from coming into direct contact with the sediment in order to avoid anoxic conditions. Egg holders consisted of pouches made of 500 μm fine nylon mesh (Dynamic Aqua-Supply Ltd., Surrey, BC) and were suspended in the jars. During water changes, fresh media was added to a second set of jars and allowed to settle for 24 h to minimize the amount of suspended solids. Egg holders were then transferred to the second set of jars containing fresh media.

Both exposures ended after 72 h, as tadpoles reached developmental NF stage 46. For each treatment, a subsample of surviving embryos ($n = 36$ –68/treatment) was fixed in 3% (w/v) formaldehyde (pH 7.0) to examine the occurrence of malformations. In addition, 8 pools of 10 embryos were sampled from each treatment and kept at –80 °C for gene expression analysis.

Malformations. Malformations were determined by visual inspection under a dissecting microscope. Different types of deformities were recorded based on the Atlas of Abnormalities for *Xenopus* spp.¹² Deformations observed included axial, eye, heart, head, and face malformations, blistering, edema, and incomplete coiling of the gut. All samples were examined by blind analysis to avoid observer bias.

RNA Isolation and cDNA Synthesis. RNA was isolated from the pooled embryos using a commercially available kit (e.Z.N.A. Total RNA Kit I, VWR International, Mississauga, ON). Prior to cDNA synthesis, downstream genomic DNA contamination was removed from the remaining samples using a deoxyribonuclease treatment (RQ1 RNase-free DNase, Promega, Madison, WI). Total cDNA was prepared from 1 μg of total RNA with the GoScript Reverse Transcription system (Promega, Madison, WI).

Real-Time RT-PCR (qPCR). Gene expression was quantified using the MX3005P real-time RT-PCR (Agilent Technologies, Santa Clara, U.S.A.). Elongation factor-1 alpha (*ef1α*) and ornithine decarboxylase (*odc*) were used as control genes to normalize the expression of target genes, as no significant differences were observed among treatments for these genes (Figure S1; S refers to Supporting Information). Three heat shock proteins (*hsp* 30, *hsp* 70, and *hsp* 90), two androgen-

Table 1. Percentage of Mortality and Malformations Occurring in *S. tropicalis* Larvae Following Exposure to DY7-Spiked Water and Sediment.^a

experiments/treatments ^b	mortality % ± SD	malformed individuals ^c % (n) ^d	malformations observed ^e n					
			axial	blistering and edema	eye	head and face	heart	gut
DY7-Spiked Water (µg/L)								
FETAX control	9.0 ± 4.1	6.8 (44)	1	0	2	1	0	2
0	11.3 ± 1.25	27.9 (43) [§]	3	3	9	1	0	2
1	9.4 ± 2.1	40.5 (37)	2	1	13	0	0	4
5	9.5 ± 2.9	43.8 (48)	4	3	16	1	0	5
7	10.0 ± 6.1	45.6 (57)	3	3	24	1	0	8
22	7.5 ± 3.5	65.0 (40)*	9	2	21	0	0	2
DY7-Spiked Sediment (µg/g)								
0	9.0 ± 4.1	25.0 (36)	4	4	6	2	0	5
1	11.3 ± 4.2	19.4 (62)	0	1	11	1	0	3
2	9.6 ± 1.7	42.6 (68)	2	1	29	0	0	1
14	16.3 ± 5.2*	43.1 (65)	3	16	8	3	1	7
209	16.3 ± 6.9*	63.0 (54)*	3	3	33	1	0	2

^aPercentage of mortality (% ± SD), percentage and number of malformed individuals (% , n), and type of malformations (n) reported are presented (n). Data were analyzed by Fisher's Exact test. For statistical significance: § is used between the FETAX control and the DY7-spiked water control and * is used between the solvent controls (0 ppm) and the treatments (p < 0.001). ^bMeasured concentrations. ^cPercentage was calculated from a subset of animals randomly collected in each treatment. ^dNumber of animals collected varies among treatments due to animal availability at the end of the exposure. ^eIncidence of malformations observed among the subset of assessed animals. Some individuals exhibited more than one type of malformations at one time.

related genes (androgen receptor, *ar* and steroid 5 alpha reductase type 2, *srd5α2*), one estrogen-related gene (estrogen receptor alpha, *era*), and two thyroid hormone related genes (thyroid hormone receptor beta, *trbeta* and deiodinase type 2, *dio2*) were measured. Sequences and primer conditions are reported in Langlois et al. 2010,⁸ except for *hsp30*, *hsp70*, and *hsp90*, where information is described in Table S1. For microarray validation, a series of genes of interest were also assessed and are presented in Table S1. Specificity of primer sets was confirmed by cloning (pGEM-T Easy Vector System, Promega, Madison, WI, U.S.A.) and by sequencing the single amplicon obtained (Robarts Research Institute, ON, Canada) as outlined in Langlois and Martyniuk, 2013.¹³

For gene expression analysis, the GoTaq qPCR Master Mix (Promega, Madison, WI, U.S.A.) that included the carboxy-X-rhodamine (CXR) reference dye and BRYT Green dye was used. Real-time RT-PCR (qPCR) cycling began with an enzyme activation step at 95 °C (15 min), followed by 40 cycles of the following: 95 °C (15 s), gene specific annealing temperature (between 58 and 62 °C for 5 s), and 72 °C (30 s). Every qPCR analysis included a negative template control sample that contained all the reaction components except for the cDNA template and a negative reverse transcriptase control sample. Standard curve efficiency (%) and the coefficient of determination of a linear regression (*R*²) were between 90 and 110% and between 0.90 and 1.00, respectively. Every sample was run in duplicate, and seven or eight samples were analyzed per treatment. Expression data were analyzed using the MxPro 4.10 software package.

Microarray Analysis. A custom annotated *S. tropicalis* 4 × 44K oligonucleotide microarray (GPL15626) has been described previously in Langlois and Martyniuk (2013)¹³ and was manufactured with Agilent Sure Print Technology (Agilent Technologies). RNA labeling, microarray hybridization, and microarray analysis were performed according to Agilent's One-Color Microarray-Gene Based Expression Analysis protocol (Version 6.5, May 2010; Agilent, Mississauga, ON). Four solvent control and four 209-µg/g-treated biological replicates

were analyzed. All microarray data from this experiment have been deposited into Gene Expression Omnibus (GSE40149). Microarray data reported in this study are MIAME compliant (<http://www.ncbi.nlm.nih.gov/geo/info/MIAME>). Complete microarray methodology can be found in the Supporting Information.

Water and Sediment Analysis. Extracts of aqueous samples were analyzed by LC-MS/MS, while extracts of sediment samples were analyzed by LC-PDA. Measured concentrations were determined using a validated analytical method and are referenced throughout this study. Complete water and sediment methodology can be found in the Supporting Information.

Data Analysis. The expression of target genes are presented as fold changes compared to the solvent controls. Mortality and qPCR data were analyzed by one-way analyses of variance (ANOVA) using TIBCO Spotfire S+ software (version 8.2). Prior to conducting the ANOVA, normality (Kolmogorov–Smirnov test) and homoscedasticity (Levene's test) were assessed. The Bonferroni post hoc test was then used to evaluate significant differences between groups. Fisher's exact test was used to analyze malformation data. Statistical analyses for microarray data were performed using JMP SAS (V9.0, Cary, NC) as per Langlois and Martyniuk (2013).¹³ Significance was set at $\alpha \leq 0.05$.

RESULTS

DY7 Concentrations. Initial concentrations of DY7 ranged from 0.003 to 22.5 µg/L for the water exposures (Table S2). In the three highest exposure treatments, measured concentrations of DY7 declined on average by a factor of 6.7 after 24 h. Conversely, during the sediment exposure experiment, aqueous concentrations of DY7 increased on average by a factor of 2 after 24 h whereas concentrations of DY7 in sediment remained largely unchanged (Table S2).

Eye Malformation Is the Most Prevalent Deformity. There was no significant difference in mortality between the FETAX control and both solvent controls used for the

exposures (Table 1). In the DY7-spiked water experiment, DY7 did not induce mortality at any of concentrations tested; however, in the sediment exposure experiment, there was a significant increase in mortality in the 14 and 209 µg/g treatments ($p = 0.01$) compared to controls. At the end of the exposures, subsets of larvae ($n = 36–68$) were analyzed for malformations (Table 1). Eye malformations, edema, and incomplete coiling of the gut were the most commonly observed malformations. There was a concentration-dependent increase in malformations with DY7 treatments, but only the highest treatment of both sets of exposures (14 and 209 µg/g) was statistically significant (Fisher's Exact test; $p < 0.001$; Table 1). Furthermore, 63% of animals in the 209 µg/g treatment exhibited at least one malformation, with malformation of the eye being the major deformity observed. In both exposure experiments, the number of malformations in the FETAX control was lower than in the solvent controls (Fisher's Exact test; $p = 0.01$ and 0.03, respectively).

DY7 Induces Heat Shock Protein mRNA. Targeted transcript analysis was used to assess the effects of DY7 on cellular stress, thyroid hormone, and on the reproductive system. No expression changes were detected for any of the genes analyzed in the DY7-contaminated water experiment. Similarly, exposure of animals to sediment spiked with DY7 did not affect the mRNA levels of *trbeta*, *dio2*, *hsp30*, and *eralpha* at any of the concentrations tested (data not shown). However, both *hsp70* and *hsp90* mRNA levels increased by 2.5 and 2.4 fold, respectively, following exposure to the highest treatments ($p < 0.01$; Figure 1B, D). For *hsp90*, a significant 1.8-fold increase was also observed in the 2 µg/g treatment ($p = 0.016$, Figure 1D). Exposure to DY7 also affected the androgen-related genes *ar* and *srd5a2*. The expression of *ar* mRNA decreased by approximately 2-fold in treated groups (Figure 1F), but it was only statistically significant in the 14 and 209 µg/g treatments ($p = 0.029$). In addition, *srd5a2* mRNA was induced by 2.6-fold at the highest concentration of DY7 (209 µg/g) ($p = 0.024$, Figure 1H). Despite an increase in malformation occurrence between the FETAX control and the solvent controls, no transcriptomics differences were observed among treatments (Figure 1).

Transcriptomics Data Suggests a Stress-Response with DY7 Exposure. Differential expression between the solvent control and DY7 treatments was observed in 10 648 probes ($p < 0.05$) and 3290 were differentially expressed at FDR = 5%. Hierarchical clustering revealed that the global gene expression profiles were different between the control and DY7 treatments (Figure S2). PCA clustering also supported a clear separation between the groups and PCA1 explained >97% of the transcriptional variation (Figure S3).

Due to the importance of cellular oxidative stress and programmed cell death in response to toxic environments, we compiled a table of transcripts involved in these processes that were differentially affected by DY7 exposure (Table S3). These transcripts were significantly induced with DY7 exposure: FCH domain only 1, PREDICTED: scavenger receptor class A member 3-like, PREDICTED: leucine-rich repeat kinase 2 were significantly decreased with DY7 exposure, while heat shock protein 90 kDa alpha (cytosolic), class A member 1, gene 1, heat shock protein 90 kDa beta (Grp94), member 1, and heat shock protein 105. The increase in heat shock proteins corroborated the qPCR data. All microarray data are provided in Supporting Information.

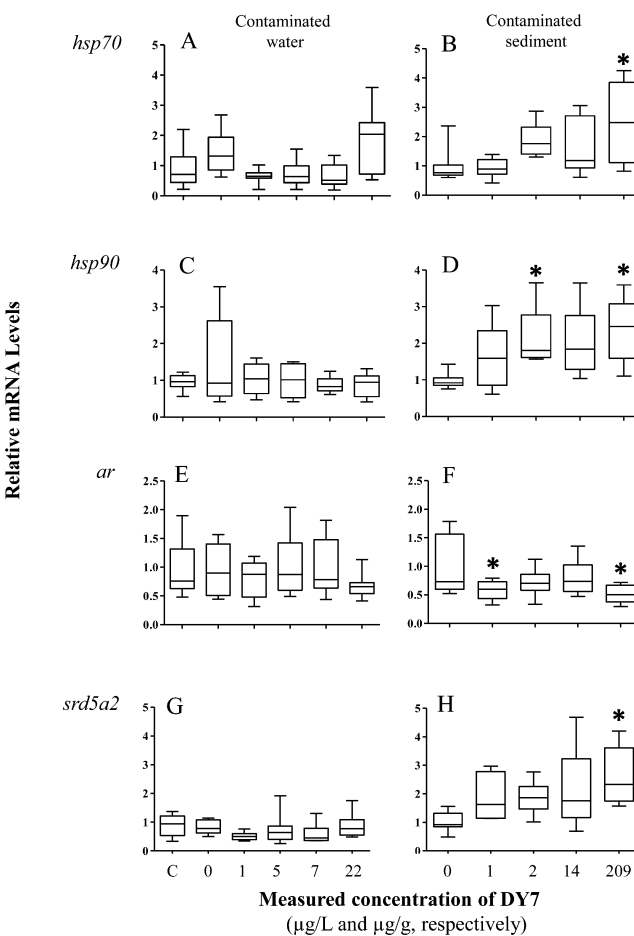


Figure 1. Expression of heat shock protein genes, *hsp70* and *hsp90* and androgen receptor (*ar*) and steroid 5 α -reductase type 2 (*srd5a2*) in *S. tropicalis* larvae after being exposed to DY7-spiked water (A, C, E, G) and DY7-spiked sediment (B, D, F, H). Expression levels were measured in whole embryos at NF stage 46. Transcript levels are normalized to the average expression of *ef1 α* and *odc*. Box plots were used to express data and minimum, 25% percentile, median, 75% percentile, and maximum are presented. One-way ANOVA was used to analyze data ($n = 7–8$; $p < 0.05$). Asterisks indicate statistically significant differences among treatments. The scales of the Y-axis vary among genes. *ar*, androgen receptor; C, FETAX control; *ef1 α* , elongation factor-1 alpha; *hsp70*, heat shock protein 70; *hsp90*, heat shock protein 90; *odc*, ornithine decarboxylase; *srd5a2*, steroid 5 α reductase type 2.

Gene Ontology, Functional Enrichment, and Subnetwork Enrichment Analysis. Functional enrichment analysis identified 35 biological processes that were altered after exposure to DY7 (Table S4). DNA replication, mitochondrial protein transport, cell cycle regulation, and mRNA transcription and processing expressed the highest ratio of the gene set change (i.e., between 20 and 30% of the genes related to these functions changed). Furthermore, unique subnetworks were also identified as being affected by DY7 treatments (Table S5; Supporting Information) including translation elongation, DNA replication initiation, retinoid metabolism, B-cell receptor signaling, blastocyst development, necrotic cell death, dopamine metabolism, and mitochondrial membrane permeability. Some interesting examples of gene networks are depicted in Figure 2. Approximately one-quarter of the transcripts involved in necrotic cell death were significantly affected by the treatment (total of 27 genes; Figure 2A). An overall reduction

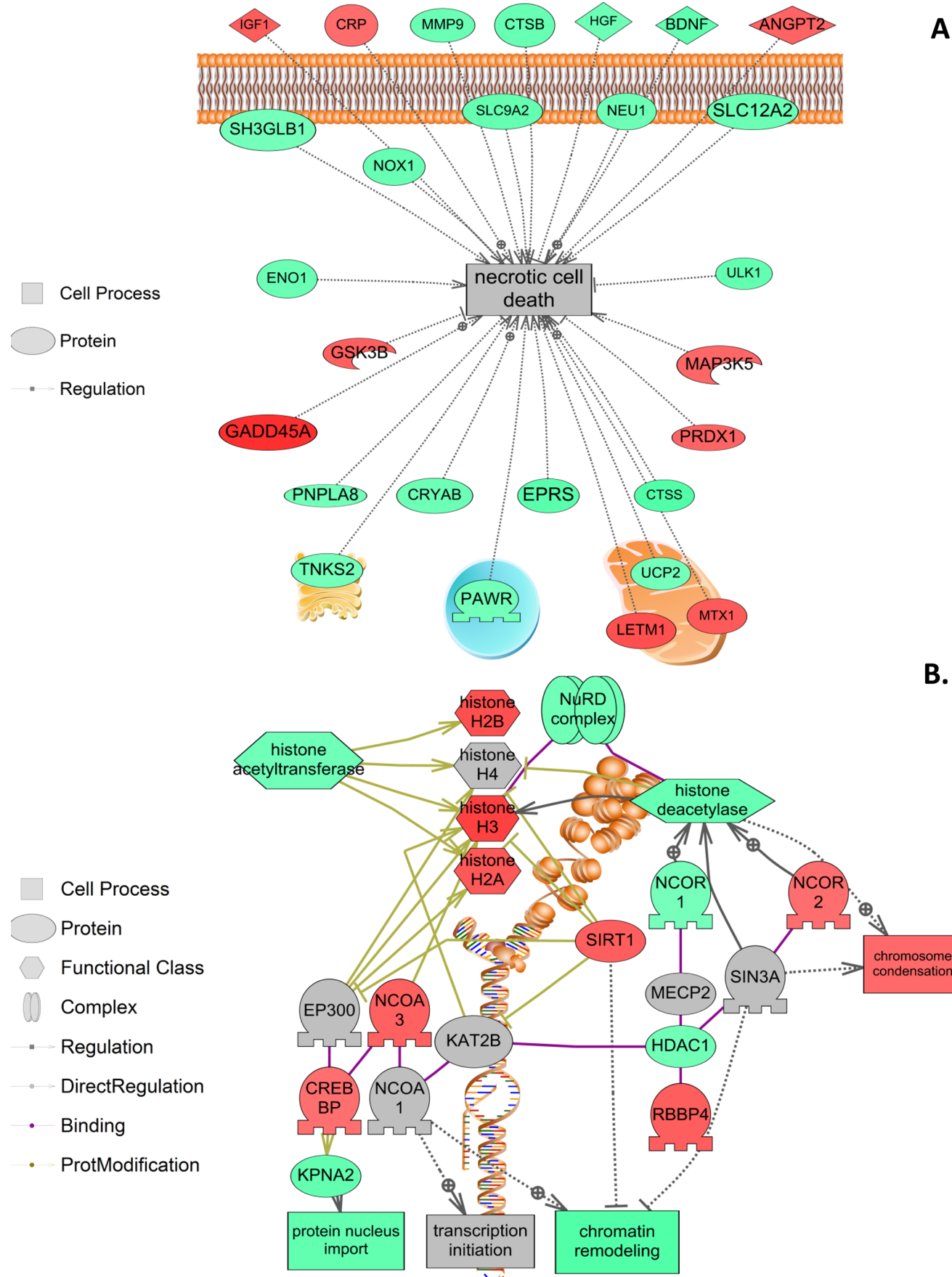


Figure 2. continued

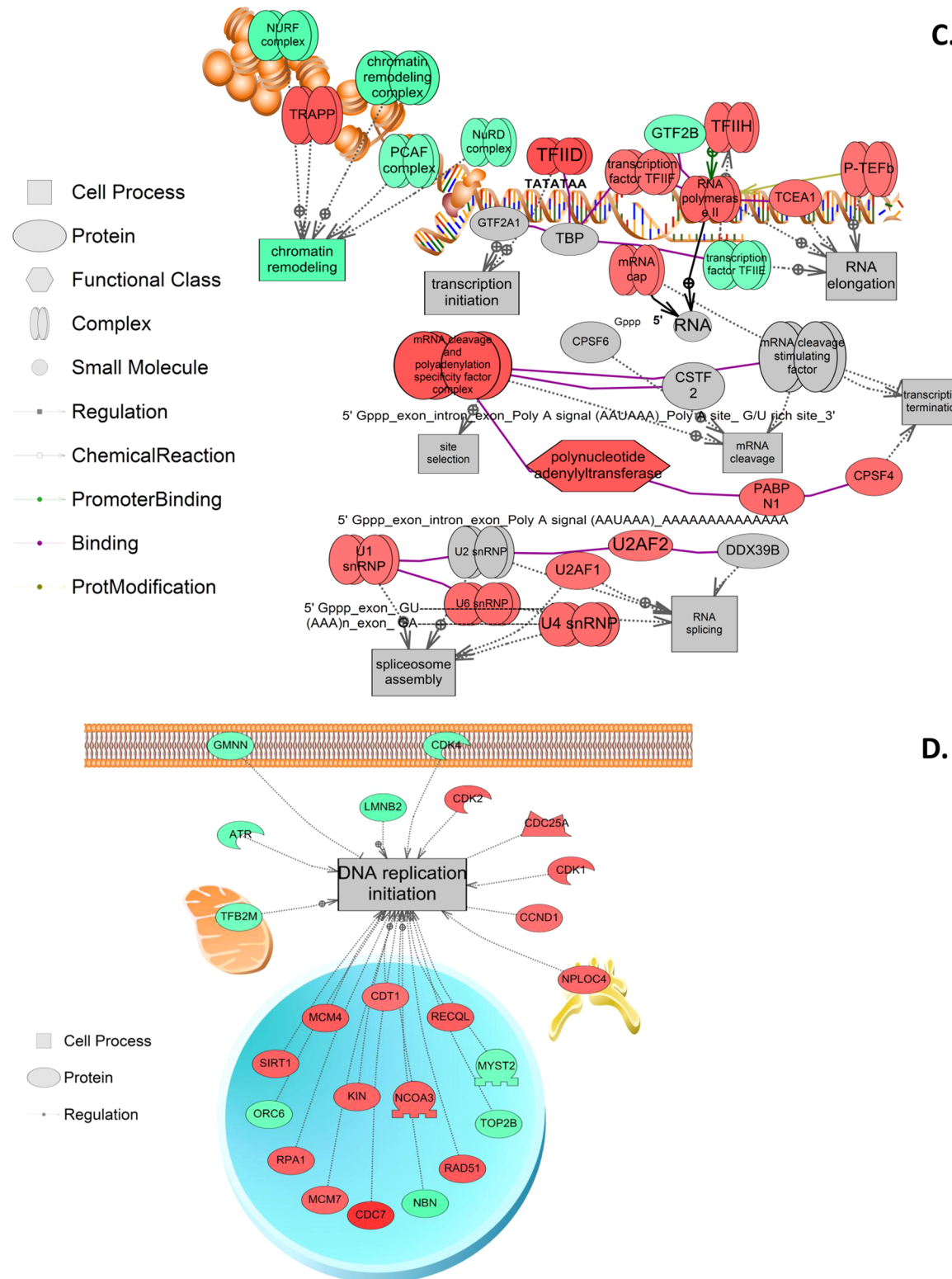


Figure 2. Subnetwork enrichment analysis identified necrotic cell death, chromosome condensation, mRNA processing, and DNA replication initiation as processes significantly altered following DY7 treatment. Red indicates that the transcript is increased, and green indicates that the transcript is decreased.

of mRNA abundance was noted in the network for necrotic cell death and mRNA levels were reduced for many genes, including mitochondrial uncoupling protein 2 (*ucp2*; mitochondrial transporter proteins), uncharacterized-51-like kinase (*ulk1*; involved in autophagy in response to starvation),

brain-derived neurotrophic factor (*bdnf*; promotes growth and survival of neurons), NADPH oxidase 1 (*nox1*; voltage-gated proton channel that generates superoxide), enolase 1 (*eno1*; multifunctional enzyme involved in glycolysis, growth control, and hypoxia tolerance, with a possible role as a tumor

suppressor), PRKC apoptosis WT1 regulator (*pawr*; pro-apoptotic protein), SH3-domain GRB2-like endophilin B (*sh3glb1*; involved in outer mitochondrial membrane dynamics), and tankyrase, TRF1-interacting ankyrin-related ADP-ribose polymerase 2 (*tnks2*; increases the activity of the destruction complex and promotes degradation of beta-catenin). Interestingly, other transcripts involved in necrotic cell death were up-regulated, including metaxin 1 (*mtx1*; essential for embryonic development by transporting proteins to mitochondria), leucine zipper-EF-hand containing transmembrane protein (*letm1*; maintains mitochondrial structure and assembly), growth arrest and DNA-damage inducible protein (*gadd45a*; responds to environmental stress, for example, stimulates DNA excision repair), and glycogen synthase kinase 3 beta (*gsk3b*; involved in glycogen metabolism with roles in cell division and survival). Descriptions of gene functions were obtained from the Weizmann Institute of Science (<http://www.genecards.org>).

Subnetwork enrichment analysis also suggested that individuals exposed to DY7 showed changes in genes associated with chromosome condensation (Figure 2B). Gene expression levels of the histone functional class representatives (e.g., histone H2A, H2B, and H3), the nuclear receptor corepressor 2 (*ncor2*), and the retinoblastoma binding protein 4 (*rnp4*) increased in the network following treatment. Similarly, mRNA levels of the nuclear receptor coactivator 3 (*ncora3*), the CREB binding protein (*crebbp*), and the sirtuin 1 (*sirt1*) mRNAs were higher in DY7 treated animals compared to those in control animals. However, histone acetyltransferases, deacetylases, and karyopherin alpha 2 (*kpn2a2*) genes were down-regulated, which led to the decrease of chromatin remodelling and protein nucleus import, two important cellular processes. The networks suggest that there is a significant up-regulation mRNA processing as well as a reduction in chromatin remodelling (Figure 2C). Several complex protein transcripts increased in the mRNA transcription and processing network, including transcription factor II D, *tffid*; transcription factor II F, *tffif*; transcription factor II H, *tffiH*; RNA polymerase II; positive transcription elongation factor b, *p-tef*b; mRNA cleavage and polyadenylation specificity factor complex; U1 spliceosomal RNA nuclear ribonucleoprotein, *u1snrnp*; U4 spliceosomal RNA nuclear ribonucleoprotein, *u4snrnp*; and U6 spliceosomal RNA nuclear ribonucleoprotein, *u6snrnp*. Other genes involved in RNA elongation (transcription elongation factor A 1, *tceal1*), pre-mRNA formation (polynucleotide adenyltransferase; poly(A) binding protein nuclear 1, *pabpn*; and cleavage and polyadenylation specific factor 4, *cpsf4*), spliceosome assembly (U2 small nuclear RNA auxiliary factor 1, *u2af1*), and RNA splicing (*u2af1* and U2 small nuclear RNA auxiliary factor 2, *u2af2*) increased in the network.

Approximately one-third of the transcriptional pathway leading to DNA replication initiation was also altered after exposure to DY7 (Figure 2D). For example, the minichromosome maintenance complex component 4 and 7 (*mcm4*, *mcm7*), cell division cycle 7 (*cdc7*), chromatin licensing and DNA replication factor 1 (*cdt1*), nuclear receptor coactivator 3 (*ncoa3*), antigenic determinant of recA protein homologue (*kin*), replication protein A1 (*rpa1*), sirtuin 1 (*sirt1*), RecQ protein-like DNA helicase Q1-like (*recql*), *rad51*, nuclear protein localization 4 homologue (*nploc4*), cyclin D1 (*ccnd1*), cyclin-dependent kinase 1 and 2 (*cdk1*, *cdk2*), and cell division cycle 25 A (*cdc25a*) were induced. Taken together, these data suggest that intracellular transcription and replication activities

may increase following exposure to different DY7 concentrations, corresponding to the point at which embryos exhibit differential survival compared to the controls. All subnetwork enrichment data are provided in Supporting Information.

Microarray validation was performed by qPCR, and the majority of the genes analyzed responded in a similar manner (i.e., direction and magnitude) to microarray data (Figure S4). For example, genes involved in apoptosis and oxidative stress (serine/threonine-protein kinase ULK1, heat shock protein 90, and caspase 7), DNA condensation (histone H2B), DNA replication (MCM4 minichromosome maintenance deficient 4 and replication protein A3), and transcription (transcription factor IIH, polypeptide 1, 62 kDa) increased in expression in both the microarray and qPCR analysis after treatment to DY7.

■ DISCUSSION

In this study, we demonstrate that the industrial disazo dye, DY7, is toxic at relatively high concentrations and that this dye can induce malformations in frog larvae when exposed to contaminated sediments. Although the aqueous concentrations of the water-only exposure were relatively higher than the aqueous concentrations of the sediment exposures, the sediment-associated DY7 was more toxic. Given that DY7 is expected to preferentially associate with sediment (based on level III fugacity modeling), it is not surprising that sediment-based toxicity was greater than water-only toxicity. Tadpoles are exposed to DY7 through different routes: (1) directly via the aqueous phase (dermal, ingestion) and (2) via the DY7 sorbed to particulates in the water column (ingestion). Azo compounds have previously been shown to induce mortality in fish and aquatic insects. The rearing of fathead minnow (*Pimephales promelas*) fry in water spiked with 0.1 ppm of Sudan Red G for 21 d demonstrated that this azo dye can be toxic to *P. promelas*. When exposed to DY7 for 21 d, 0.025 ppm was sufficient in concentration to decrease the survival of *P. promelas* fry.¹⁴ In contrast, Sudan Red G was not toxic to mayflies (*Hexagenia spp.*) larvae when exposed to spiked sediment for 21 d.¹ The authors suggested that Sudan Red G was either not absorbed by the digestive tract of *Hexagenia spp.* or that the azo bond was not cleaved; therefore, no toxic metabolites were produced. A study conducted in Wood frog (*Rana sylvatica*) found that lethal and sublethal effects of PCB-contaminated sediment were more pronounced in tadpoles when there was presence of sediment,¹⁵ suggesting that perhaps DY7 metabolites are also more concentrated and bioactive in the sediment compared to a waterborne exposure. Azo dyes are generally water insoluble. To the best of the authors' knowledge, no reports have been made concerning the concentration of DY7, in actual sediments or receiving waters. We estimated the log K_{ow} of DY7 to be 6.3 using a Level III fugacity model,¹⁶ indicating that azo dyes will be dominantly found in sediment and bound to particulates at levels that would be orders of magnitude greater than those found in overlying waters. Consequently, we suggest that the exposure routes of *S. tropicalis* larvae to DY7 or similar azo and benzidine compounds are through ingestion (as these frog larvae start feeding at NF stage 46) and through dermal contact of contaminated particulates in the water column.

An increase in the presence of malformations was observed in the 209 $\mu\text{g/g}$ DY7 treatment relative to the controls, with more than 60% of the larvae exhibiting malformations. Malformation of the eye was the major deformity detected after exposure, followed by incomplete coiling of the gut, and

blistering/edema. It is well documented that retinoid acid plays an important role in eye development. It has been shown that certain environmental pollutants (e.g., tributyltin) bind to retinoid X receptors (RXR), which has been suggested to interfere with retinoid acid signaling leading to eye malformations in frogs.^{17,18} Interestingly, our study found that retinoid metabolism was one of the pathways that was significantly repressed at the transcriptomics level. Lupo et al. (2006) also demonstrated the roles for the retinoid acid receptor in eye patterning and that receptor inhibition resulted in a slight dorsalization of the eyes.¹⁹ In mammals, retinoid acid receptor mutants exhibited eye abnormalities similar to fetuses deprived of vitamin A.²⁰ Furthermore, retinoic acid disruption has been shown to lead to other types of deformities in later stages of development. For example, studies have demonstrated that the alteration of retinoid acid levels resulted in limb malformations.^{21,22} All together, this data suggests that DY7 induces eye malformations in the developing frog embryo, and the observed alteration of the retinoid metabolism by DY7 could also lead to further limb deformities in later stages of the frog life cycle.

Some of the toxicity or teratogenicity of azo dyes may arise from degradation products and not solely from the parent molecules. The azo bond can be reductively split into aromatic amines, or transformed via a benzidine rearrangement to form benzidines (e.g., R-N-Ar-Ar-N-R').²³ Azo bonds may be reductively split through biodegradation and biotransformation caused by biotic processes such as enzymatic action (e.g., azoreductases and microsomal enzyme),^{24,25} or by abiotic processes such as thermal and photodegradation and transformation.^{26,27} Benzidine compounds have been shown to be genotoxic and mutagenic,²⁸ and both azos and their degradation products can be activated metabolically to form reactive electrophilic intermediates that covalently bind DNA.²⁹ Although the carcinogenicity of azo dyes in humans is uncertain, these compounds have been shown to induce cancers, malformations, and dysfunction of reproductive organs in rats and mice (especially in the male reproductive system³⁰) and to be genotoxic in male rats.³¹ Thus, there is a wide range of reported adverse effects due to exposure to azo dyes. Evidence suggests that the degradation of azo dyes may form free radicals³² and increase lipid peroxidation and reactive oxygen species.³³ The putative role of such metabolites is the focus of ongoing investigation in our laboratories.

Eukaryotic cells preserve their genomic and cellular integrity against environmental stressors (e.g., UV-radiation, chemicals, reactive oxygen species) using cellular protection machinery³⁴ (e.g., DNA repair, antioxidation). A number of genes associated with cellular protection were induced after exposure to DY7. Increases in *hsp70*, *hsp90*, and *hsp105* mRNAs suggest that treated frog larvae were experiencing cellular stress. Heat shock proteins are classic biomarkers of a generalized stress response and are chaperone proteins that have roles in stabilizing nascent and denatured polypeptides during cytotoxic aggregations, among other functions.^{35–37} For example, heat shock protein 70 plays an essential role in (1) maintaining protein integrity, (2) facilitating the folding of the hormone-binding domain to activate steroid receptors, (3) protecting the organisms from oxidative stress by preventing the irreversible loss of vital proteins, and (4) modulating immune responses.^{38–41} Several ecotoxicological studies have demonstrated a positive correlation between increased heat shock protein expression and exposure to chemical stressors (e.g., *hsp30*, *X. laevis*;⁴² *hsp70*,

Propocentrum minimum;⁴³ *hsp70*, *Chironomus riparius*;⁴⁴ *hsp70*, *S. tropicalis*,⁴⁵ *hsp70* and *hsp90*, *Gobiocypris rarus*⁴¹). In a similar study, the azo dye Bismarck brown Y has also resulted in a significant increase of *hsp70* mRNA in *S. tropicalis* larvae when exposed to a high concentration of Bismarck brown Y-spiked sediment.⁴⁵ The expression of heat shock proteins increases to protect the cell and increase the stress threshold. We suggest that a similar phenomenon is occurring in frog larvae exposed to azo dyes.

Exposure to chemicals present in the environment can lead to mortality, induction of morphological deformities, and cellular damage. However, there remain several adverse effects such as genotoxic and epigenetic effects for which mechanisms of action remain to be fully characterized.⁴⁶ Global gene expression analysis can offer insight into these underlying mechanisms. It is important to note that microarray data were collected at a single time point at the termination of the exposure. Thus, molecular responses and gene networks identified here will require additional experimental validation at the molecular and physiological level over different exposure durations. Despite this limitation, this data generates new hypotheses regarding the action of azo dyes in vertebrates and identify related molecular pathways that correspond to morphological end points (i.e., retinoic acid metabolism and eye formation). Indeed, our transcriptomics data shows that processes related to histone acetyltransferases are affected by DY7. Histone acetyltransferases (HAT) are important enzymes involved in nucleosome modeling and allow gene transcription and DNA repair to occur.⁴⁷ Cancer research has demonstrated that inhibition of HAT leads to accumulation of DNA damage, ultimately increasing the expression of genes involved in the DNA damage response, and results in cellular apoptosis.³⁴ Interestingly, our microarray data demonstrates that DY7 decreased HAT expression, which is consistent with the increase in the expression of genes involved in DNA damage. It is well documented that chromosome condensation can lead to transcription repression and that aberrant condensation of DNA can prevent transcription to occur. For example, exposure to nickel compounds has been associated with carcinogenicity and results in the remodelling of euchromatin at the euchromatin-heterochromatin junction, thus repressing the expression of genes.⁴⁸ DY7-treated frog larvae exhibited increases in histone transcripts (*h2a*, *h2b*, and *h3*) and an overall augmentation in chromosome condensation.

Azo compounds have also been shown to interfere with male reproductive status in rodents. Mice and rats exposed to untreated textile wastewater containing azo dyes exhibited altered male characteristics (i.e., reduced reproductive organ weight, altered spermatogenesis, induced sperm abnormalities, and reduced sperm counts). It has been suggested that the effects could be explained by the suppression of both the synthesis and the secretion of androgen hormones.³⁰ A disruption of *ar* mRNA levels by DY7 could also have detrimental effects on sex differentiation and development. In the present study, the expression of two androgen-related genes was altered by DY7 (*srd5α2* and *ar*). The highest concentration of DY7 significantly increased *srd5α2* mRNA levels. This enzyme is involved in androgen biosynthesis by converting testosterone into 5α-dihydrotestosterone (5α-DHT).⁴⁹ Furthermore, DY7 treatment resulted in decreased *ar* mRNA. As male sexual differentiation is entirely androgen-dependent, *ar* is essential for binding 5α-DHT.⁵⁰ The decrease in *ar* mRNA may be explained by a putative lack of androgens that self-

regulate their own receptor. This is the first report that DY7 can interfere with the male reproductive status in frogs. Further research on the effects of DY7 on hormone levels would allow for a better understanding of the functional effects of DY7 on the androgen axis.

The aims of this study were to determine the toxicity and sublethal effects of DY7 and to investigate its mechanisms of action in frogs. This work is important as the full range of azo dyes in the Canadian environment has not been completely identified. Our results demonstrate that a sediment exposure route to high concentrations of DY7 led to increase in mortality and malformation occurrence in *S. tropicalis* larvae. We demonstrated that DY7 induces cellular stress and interferes with both androgen signaling and biosynthesis in developing *S. tropicalis*. This study is the first to investigate in depth the mechanisms of action of azo dyes and to identify cell processes that may be susceptible in animals exposed to DY7.

ASSOCIATED CONTENT

Supporting Information

Additional tables, figures, and methodologies. This material is available free of charge via the Internet at <http://pubs.acs.org>.

AUTHOR INFORMATION

Corresponding Author

*Phone: +1 613 541 6000 ext. 3621. Fax: +1 613 542 9489. E-mail: valerie.langlois@rmc.ca.

Present Address

[#]Christopher J. Martyniuk: Center for Environmental and Human Toxicology & Department of Physiological Sciences, University of Florida, Gainesville, FL 32611, United States

Notes

The authors declare no competing financial interest.

ACKNOWLEDGMENTS

The authors thank Almira Siew and Grant Norman for laboratory assistance, Diana Flood for help with animal care (from RMCC), and Danielle Milani (from Environment Canada) for collecting sediment in Lake Erie. This work was supported by the Science and Risk Assessment Directorate (2011-12) of Environment Canada to S.d.S. and V.S.L., Ecotoxicology and Wildlife Division to S.d.S., NSERC Discovery Grant to V.S.L. and C.J.M., and Canada Research Chair to C.J.M.

REFERENCES

- (1) Legault, D. M. Determining the toxicity of Sudan Red G using the benthic invertebrates *Hexagenia* spp. and *Tubifex tubifex*. University of Waterloo, Waterloo, 2010.
- (2) Zhou, M.; He, J. Degradation of azo dye by three clean advanced oxidation processes: Wet oxidation, electrochemical oxidation, and wet electrochemical oxidation. A comparative study. *Electrochim. Acta* **2007**, *53*, 1902–1910.
- (3) Nam, S.; Renganathan, V. Non-enzymatic reduction of azo dyes by NADH. *Chemosphere* **2000**, *40*, 351–357.
- (4) Shaul, G. M.; Holdsworth, T. J.; Dempsey, C. R. Fate of water soluble azo dyes in the activated sludge process. *Chemosphere* **1991**, *22*, 107–119.
- (5) Olcay Topaç, F.; Dindar, E.; Uçaroğlu, S.; Başkaya, H. S. Effect of a sulfonated azo dye and sulfanilic acid on nitrogen transformation processes in soil. *J. Hazard. Mater.* **2009**, *170*, 1006–1013.
- (6) Maguire, R. J.; Tkacz, R. J. Occurrence of dyes in the Yamaska River, Québec. *Water Pollut. Res. J. Can.* **1991**, *26* (2), 145–161.
- (7) Standard guide for conducting the frog embryo teratogenesis assay—*Xenopus* (FETAX). ASTM, American Society for Testing and Materials: Philadelphia, 1998; E1439-98.
- (8) Langlois, V. S.; Duarte-Guterman, P.; Ing, S.; Pauli, B. D.; Cooke, G. M.; Trudeau, V. L. Fadrozole and finasteride exposures modulate sex steroid- and thyroid hormone-related gene expression in *Silurana* (*Xenopus*) *tropicalis* early larval development. *Gen. Comp. Endocrinol.* **2010**, *166*, 417–427.
- (9) Fort, D. J.; Rogers, R. L.; Thomas, J. H.; Buzzard, B. O.; Noll, A. M.; Spaulding, C. D. Comparative sensitivity of *Xenopus tropicalis* and *Xenopus laevis* as test species for the FETAX model. *J. Appl. Toxicol.* **2004**, *24*, 443–457.
- (10) Changez, M.; Koul, V.; Krishna, B.; Kumar Dinda, A.; Choudhary, V. Studies on biodegradation and release of gentamicin sulphate from interpenetrating network hydrogels based on poly(acrylic acid) and gelatin: *in vitro* and *in vivo*. *Biomaterials* **2004**, *25*, 139–146.
- (11) Milani, D.; Intini, K. Toxicity of disperse dyes to the mayfly *Hexagenia* spp. and oligochaete worm *Tubifex tubifex* in spiked sediment exposures. *Environmental Canada: Internal Report* **2013**, *31*.
- (12) Bantle, J. A.; Dumont, J. N.; Finch, R. A.; Linder, G.; Fort, D. J. *Atlas of Abnormalities: A Guide for the Performance of FETAX*, 2nd ed.; Oklahoma State University: Stillwater, OK, 1998.
- (13) Langlois, V. S.; Martyniuk, C. J. Gene regulatory networks involved in early embryonic *Silurana tropicalis* development. *Mech. Dev.* **2013**, *130*, 304–322.
- (14) Parrott, J. L.; Blunt, B.; Regan, C.; Palabricia, V.; Balakrishnan, V. *Sublethal toxicity of CMP dyes to fish*. Unpublished data.
- (15) Savage, W. K.; Quimby, F. W.; DeCaprio, A. P. Lethal and sublethal effects of polychlorinated biphenyls on *Rana sylvatica* tadpoles. *Environ. Toxicol. Chem.* **2002**, *21*, 168–74.
- (16) Mackay, D. *Multimedia Environmental Models: The Fugacity Approach*, 2nd ed.; Lewis Publishers: Boca Raton, FL, 2001.
- (17) Grün, F.; Watanabe, H.; Zamanian, Z.; Maeda, L.; Arima, K.; Cubacha, R.; Gardiner, D. M.; Kanno, J.; Iguchi, T.; Blumberg, B. Endocrine-disrupting organotin compounds are potent inducers of adipogenesis in vertebrates. *Mol. Endocrinol.* **2006**, *20*, 2141–2155.
- (18) Guo, S.; Qian, L.; Shi, H.; Barry, T.; Cao, Q.; Liu, J. Effects of tributyltin (TBT) on *Xenopus tropicalis* embryos at environmentally relevant concentrations. *Chemosphere* **2010**, *79*, 529–533.
- (19) Lupo, G.; Harris, W. A.; Lewis, K. E. Mechanisms of ventral patterning in the vertebrate nervous system. *Nat. Rev. Neurosci.* **2006**, *7*, 103–114.
- (20) Ross, A. C. Vitamin A and retinoids. In *Modern Nutrition in Health and Disease*, 9th ed.; Shils, M. F., Olson, J. A., Shike, M., Ross, A. C.; Eds; William & Wilkins: Baltimore, 2000; pp 305–327.
- (21) Lee, G. S.; Kochhar, D. M.; Collins, M. D. Retinoid-induced limb malformations. *Curr. Pharm. Des.* **2004**, *10*, 2657–2699.
- (22) Loeffler, I. K.; Stocum, D. L.; Fallon, J. F.; Meteyer, C. U. Leaping lopsided: a review of the current hypotheses regarding etiologies of limb malformations in frogs. *Anat. Rec.* **2001**, *265*, 228–245.
- (23) Chung, K. - T.; Cerniglia, C. E. Mutagenicity of azo dyes: Structure–activity relationships. *Mutat. Res.* **1992**, *277*, 201–220.
- (24) USEPA. Office of Prevention, Pesticides, and Toxic Substances. Dyes derived from benzidine and its congeners (DCB) Action plan. U.S. Environmental Protection Agency, Office of Prevention, Pesticides, and Toxic Substances: Washington DC, 2010.
- (25) Golka, K.; Kopps, S.; Myslak, Z. W. Carcinogenicity of azo colorants: Influence of solubility and bioavailability. *Toxicol. Lett.* **2004**, *151*, 203–210.
- (26) Øllgaard, H.; Frost, L.; Galster, J.; Hansen, O. C. Survey of azo-colorants in Denmark: Consumption, use, health and environmental aspects. Ministry of Environment and Energy, Danish Environmental Protection Agency: Copenhagen (DK), 1998.
- (27) Weber, E. J.; Adams, R. L. Chemicals and sediment-mediated reduction of the azo dye Disperse Blue 79. *Environ. Sci. Technol.* **1995**, *29*, 1163–1170.

- (28) Claxton, L. D.; Hugues, T. J.; Chung, K. T. Using base-specific *Salmonella* tester strains to characterize the types of mutation induced by benzidine and benzidine congeners after reductive metabolism. *Food Chem. Toxicol.* **2001**, *39*, 1253–1261.
- (29) Brown, M. A.; DeVito, S. C. Predicting azo dye toxicity. *Crit. Rev. Environ. Sci. Technol.* **1993**, *23*, 249–324.
- (30) Suryavathi, V.; Sharma, S.; Sharma, S.; Saxena, P.; Pandey, S.; Grover, R.; Kumar, S.; Sharma, K. P. Acute toxicity of textile dye wastewaters (untreated and treated) of Sangamer on male reproductive systems of albino rats and mice. *Reprod. Toxicol.* **2005**, *19*, 547–556.
- (31) Abd El-Rahim, W. M.; Khalil, W. K. B.; Eshak, M. Genotoxicity studies on the removal of a direct textile dye by a fungal strain, *in vivo*, using micronucleus and RAPD-PCR techniques on male rats. *J. Appl. Toxicol.* **2008**, *28*, 484–490.
- (32) Nakayama, T.; Kimura, T.; Kodama, M.; Nagata, C. Generation of hydrogen peroxide and superoxide anion from active metabolites of naphthylamines and aminoazo dyes: Its possible role in carcinogenesis. *Carcinogenesis* **1983**, *4*, 765–769.
- (33) Gao, Y.; Li, ; Shen, J.; Yin, H.; An, X.; Jin, H. Effect of food azo dye tartrazine on learning and memory functions in mice and rats, and the possible mechanisms involved. *J. Food Sci.* **2011**, *76*, T125–T129.
- (34) Rossetto, D.; Truman, A. W.; Kron, S. J.; Côté, J. Epigenetic modifications in double strand break DNA damage signaling and repair. *Clin. Cancer Res.* **2010**, *16*, 4543–4552.
- (35) Stephanou, A.; Latchman, D. S. Transcriptional modulation of heat-shock protein gene expression. *Biochem. Res. Int.* **2011**, *1*–8.
- (36) Gupta, S. C.; Sharma, A.; Mishra, M.; Mishra, R. K.; Chowdhuri, D. K. Heat shock proteins in toxicology: How close and how far? *Life Sci.* **2010**, *86*, 377–384.
- (37) Fink, A. L. Chaperone-mediated protein folding. *Physiol. Reviews* **1999**, *79*, 425–449.
- (38) Jiang, J.; Shi, Y.; Shan, Z.; Yang, L.; Wang, X.; Shi, L. Bioaccumulation, oxidative stress, and HSP70 expression in *Cyprinus carpio* L. exposed to microcystin-LR under laboratory conditions. *Comp. Biochem. Physio. Part C* **2012**, *155*, 483–490.
- (39) Martini, F.; Fernández, C.; Tarazona, J. V.; Pablos, M. V. Gene expression of heat shock protein 70, interleukin-1 β and tumor necrosis factor α as tools to identify immunotoxic effects on *Xenopus laevis*: A dose-response study with benzo[a]pyrene and its degradation products. *Environ. Pollut.* **2012**, *160*, 28–33.
- (40) Lu, S.; Tan, Z.; Wortman, M.; Lu, S.; Dong, Z. Regulation of heat shock protein 70-1 expression by androgen receptor and its signalling in human prostate cancer cells. *Int. J. Oncol.* **2010**, *36*, 459–467.
- (41) Yang, L.; Zha, J.; Zhang, X.; Li, W.; Li, Z.; Wang, Z. Alterations in mRNA expression of steroid receptors and heat shock proteins in the liver of rare minnow (*Grobioyparis rarus*) exposed to atrazine and p,p'-DDE. *Aq. Toxicol.* **2010**, *98*, 381–387.
- (42) Woolfson, J. P.; Heikkila, J. J. Examination of cadmium-induced expression of the small heat shock protein gene, hsp30, in *Xenopus laevis* A6 kidney epithelial cells. *Comp. Biochem. Physiol. Part A* **2009**, *152*, 91–99.
- (43) Guo, R.; Ki, J.-S. Evaluation and validation of internal control genes for studying gene expression in the dinoflagellate *Prorocentrum minimum* using real-time PCR. *Eur. J. Protistol.* **2012**, *48*, 199–206.
- (44) Morales, M.; Planelló, R.; Martínez-Paz, P.; Herrero, O.; Cortés, E.; Martínez-Guitarte, J. L.; Morcillo, G. Characterization of *Hsp70* gene in *Chironomus riparius*: Expression in response to endocrine disrupting pollutants as a marker of ecotoxicological stress. *Comp. Biochem. Physiol. C. Toxicol. Pharmacol.* **2011**, *153*, 150–158.
- (45) Soriano, J. J.; Mathieu-Denoncourt, J.; Norman, G.; de Solla, S. R.; Langlois, V. S. Toxicity of the azo dyes Acid Red 97 and Bismarck Brown Y to Western clawed frog (*Silurana tropicalis*). *Environ. Sci. Pollut. Res.* **2014**, DOI: 10.1007/s11356-013-2323-4.
- (46) Head, J. A.; Dolinoy, D. C.; Basu, N. Epigenetics for ecotoxicologists. *Environ. Toxicol. Chem.* **2012**, *31*, 221–227.
- (47) Vandegehuchte, M. B.; Janssen, C. R. Epigenetics and its implications for ecotoxicology. *Ecotoxicology* **2011**, *20*, 607–624.
- (48) Ellen, T. P.; Kluz, T.; Harder, M. E.; Xiong, J.; Costa, M. Heterochromatinization as a potential mechanism of nickel-induced carcinogenesis. *Biochemistry* **2009**, *48*, 4626–4632.
- (49) Langlois, V. S.; Zhang, D.; Cooke, G. M.; Trudeau, V. T. Evolution of steroid 5 α -reductases and comparison of their function with 5 β -reductase. *Gen. Comp. Endocrinol.* **2010**, *166*, 489–497.
- (50) Luccio-Camelo, D. C.; Prins, G. S. Disruption of androgen receptor signalling in males by environmental chemicals. *J. Steroid Biochem. Mol. Biol.* **2011**, *127*, 74–82.